

See discussions, stats, and author profiles for this publication at: <https://www.researchgate.net/publication/252299681>

# Wave slope measurement using imaging polarimetry

ARTICLE *in* PROCEEDINGS OF SPIE - THE INTERNATIONAL SOCIETY FOR OPTICAL ENGINEERING · MAY 2009

Impact Factor: 0.2 · DOI: 10.1117/12.819031

---

READS

11

5 AUTHORS, INCLUDING:



[Howard Schultz](#)

University of Massachusetts Amherst

61 PUBLICATIONS 594 CITATIONS

[SEE PROFILE](#)

# Wave Slope Measurement Using Imaging Polarimetry

J. Larry Pezzaniti, David Chenault, Mike Roche, John Reinhardt  
Polaris Sensor Technologies

Howard Schultz  
University of Massachusetts

## Abstract

Imaging polarimetry can be used to accurately measure wave slopes of ocean waves in real time. An imaging polarimeter measures the polarization ellipse, and hence the degree of polarization and its orientation, by acquiring a number of images each of which analyzes a different polarization state. By knowing the geometry of the camera and its relationship to the sea surface and the measured polarization quantities, the wave slope can be extracted. We have developed and tested such an instrument with good results. For this talk, the four camera imaging polarimeter operating in the visible at 60 frames per second will be presented. The polarimeter design, calibration procedures, and the data from several data acquisition programs using the instrument will be presented.

## 1. Introduction

Light reflected from the surface of water is partially polarized. The light's degree of polarization and orientation of its polarization ellipse depend on the wave-slope, wave-slope orientation relative to the observer, the polarization state of solar or sky shine reflecting from the water, and the refractive index of the top layer(s) of the water. The polarization state may also depend on the upwelling light resulting from sun-light and sky shine scattering from material below the water surface then refracting out of the water in the direction of the observer. Because the s- and p- reflection/refraction coefficients from the Fresnel equations depend on angle of incidence, the polarization state of light reflected from and or refracted out of the water can be related to the orientation and magnitude of the wave-slopes. If the light emanating from the surface of the water is dominated by surface reflections i.e. upwelling light can be ignored, and the degree of polarization of the sky-shine is negligible, then the relationship between polarization and wave-slope is straightforward.

This paper presents a visible wavelength imaging polarimeter designed to measure polarization images from water surface. It presents calibration data, laboratory data and data sets taken of the ocean surface from Scripps Pier in LaJolla, California in January 2008. Data reduction of the data sets assumes water surface reflection only and unpolarized sky-shine. For the conditions of the test presented here and many situations, this is a good assumption.

The imaging polarimeter has the spatial resolution and speed necessary to measure short wind waves, capillary waves and small scale breaking waves that ride on top of gravity waves. Small wind waves, capillary waves and small breaking waves have

periods on the order of 1cm or less, a frequency of up to 5 Hz and a slope range of +/- 45 degrees. These waves can ride on top of long gravity waves (ocean swell) which can move as fast as 20m/sec. The desired slope resolution for measuring the water waves is 1 degree. Consideration of the speed of the changes of the wave-slope and desired wave-slope resolution leads to a required stop-action integration time on the order of 1 or 2 milliseconds.

The speed requirement was one of the principle drivers for the imaging polarimeter design. First, because the image is captured in 1 or 2 ms, there is not enough time to acquire multiple polarization images sequentially in time. Instead, the imaging polarimeter must capture all the required polarization images simultaneously. Second, because of the short integration time, the lens system must be fast (low f/#) to collect sufficient light. Third, the wavelength bandwidth must be wide enough to collect enough light to support the short integration time, but not so wide that the relationship between polarization and wave-slope becomes intractable. Fourth, the speed of the imaging polarimeter had to be at least 60 frames per second so that the evolution of the waves could be tracked. An additional requirement was set to make the imaging polarimeter a complete Stokes imaging polarimeter so that circularly polarized light could be measured.

The following table gives the specifications for the Four Camera Stokes Imaging Polarimeter.

Table 1. Specifications for Four Camera Stokes Imaging Polarimeter

<i>Parameter</i>	<i>Specification</i>
Operating Wavelength	430-630nm
FOV	4.8 x 3.6 degrees
Pixel Resolution	782 x 582
Max Frame Rate	60 frames/sec
Normalized Stokes accuracy	0.01
Integration time:	1 msec – 10msec
Working Distance	1 meter - infinity
Objective Focal Length	75mm
Selectable F/#	2.8, 3.2, 4, 5.6, 8 16, 32
Pixel size	8.3µm square
IFOV @ 8 meters	1.5mm

Section 2 will present the imaging polarimeter design that meets all of these requirements. Section 3 describes the calibration of the system and discusses the data sets from measurements of the ocean surface taken in LaJolla. Finally Section 4 provides some concluding remarks.

## 2. Imaging Polarimeter Design

**Figure 1** shows the design for the imaging polarimeter that meets the requirements given in the introduction. The system makes use of a beam splitter assembly that routes the light from an object point based on the object point's polarization state onto corresponding pixels of 4 CCDs. The first element of the beam

splitter block is a partially polarizing beam splitter cube. The cube transmits approximately 80% p-polarized light and 20% s-polarized light. The cube reflects 20% p-polarized light and 80% s-polarized light. Light that is transmitted through partial polarizing beam splitter passes through a  $\lambda/2$  retarder oriented at 22.5 degree angle (see coordinate system in **Figure 1**), then the resultant p-polarized component is transmitted through a polarizing beam splitter onto CCD 1 and the s-polarized component is reflected onto CCD 2. The light reflected from the partial polarizing beam splitter is transmitted through a  $\lambda/4$  retarder oriented at 45 degrees, then the resultant p-polarized component is transmitted through a polarizing beam splitter onto CCD 3 and the s-polarized component is reflected from the polarizing beam splitter onto CCD 4.

The optical path lengths through the beam splitter assembly to CCDs 1 through 4 are identical. Also, note that none of the elements of the beam splitter assembly have optical power. Therefore each of the four images has precisely the same magnification, distortion and MTF across the entire FOV, making precise image registration possible without image morphing. Image shifts are necessary however because the CCDs cannot be held to within 1/10<sup>th</sup> pixel registration.

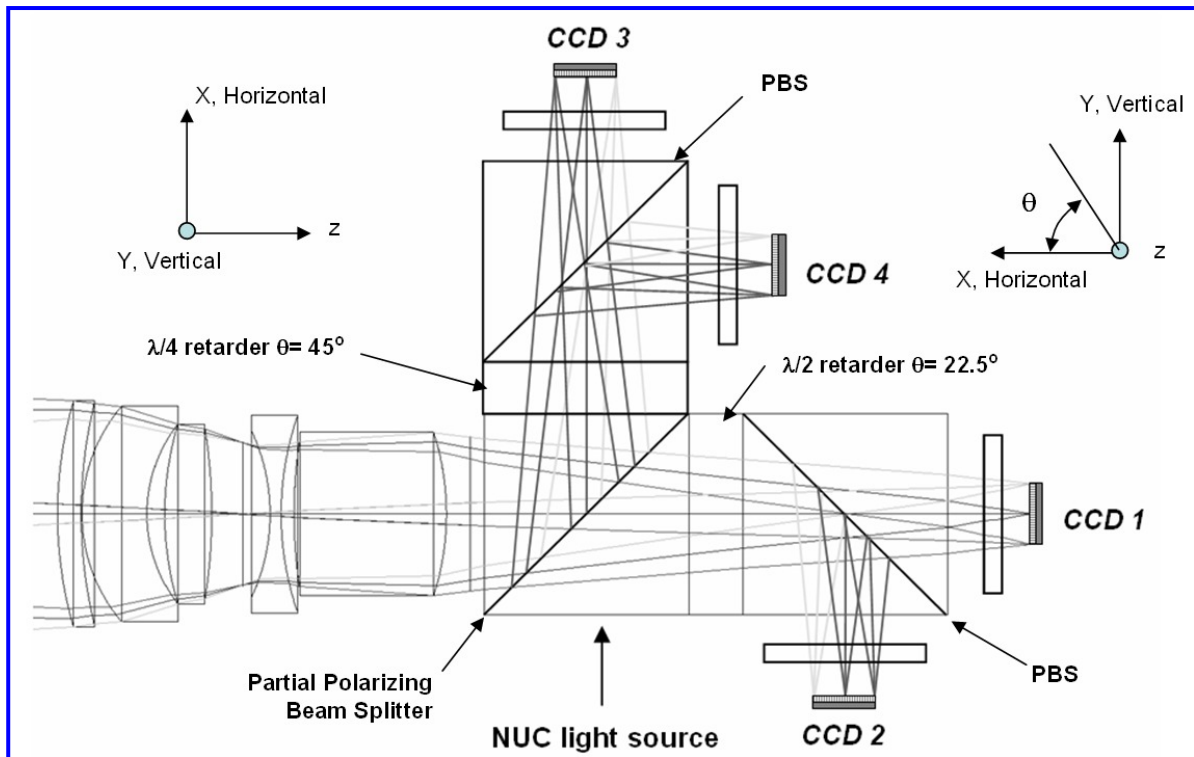


**Figure 1** Schematic of Full Stokes Imaging Polarimeter.

A Stokes vector is computed for each pixel of the image from a weighted sum of the four ADU values from corresponding pixels of the images from the 4 CCDs. The Stokes vector is defined as,

$$\mathbf{S} = \begin{bmatrix} \mathbf{H} + \mathbf{V} \\ \mathbf{H} - \mathbf{V} \\ \mathbf{45} - \mathbf{135} \\ \mathbf{R} - \mathbf{L} \end{bmatrix} \quad (1)$$

where  $\mathbf{H}$ ,  $\mathbf{V}$ ,  $\mathbf{45}$ ,  $\mathbf{135}$  are the intensities in the horizontal, vertical, 45 degree, 135 degree linearly polarized states (see coordinate system in Figure 1) and  $\mathbf{R}$  and  $\mathbf{L}$  are the intensity in the right and left circularly polarized states.

The CCD arrays are insensitive to polarization state. Therefore the CCD arrays measure the top row of the resultant Mueller matrices dotted with the incident Stokes vector<sup>1</sup>. The top row of a path's Mueller matrix is called its analyzer vector  $\mathbf{A}$  (row vector). Paths 1 through 4 analyzer vectors are given by

$$\begin{aligned} \mathbf{A}_{\text{path 1}} &= [0.25 \quad 0.15 \quad -0.20 \quad 0.00] \\ \mathbf{A}_{\text{path 2}} &= [0.25 \quad 0.15 \quad 0.20 \quad 0.00] \\ \mathbf{A}_{\text{path 3}} &= [0.25 \quad -0.15 \quad 0.00 \quad -0.20] \\ \mathbf{A}_{\text{path 4}} &= [0.25 \quad -0.15 \quad 0.00 \quad 0.20] \end{aligned} \quad (2)$$

Combining the analyzer vectors as rows in a 4x4 matrix forms a measurement matrix. The measured intensities at four corresponding pixels for the imaging polarimeter is determined by the measurement matrix dotted with the incident Stokes vector,

$$\mathbf{I} = \begin{bmatrix} i_{\text{path 1}} \\ i_{\text{path 2}} \\ i_{\text{path 3}} \\ i_{\text{path 4}} \end{bmatrix} = \mathbf{A} \bullet \mathbf{S} = \begin{bmatrix} 0.25 & 0.15 & -0.20 & 0.00 \\ 0.25 & 0.15 & 0.20 & 0.00 \\ 0.25 & -0.15 & 0.00 & -0.20 \\ 0.25 & -0.15 & 0.00 & 0.20 \end{bmatrix} \bullet \begin{bmatrix} s_0 \\ s_1 \\ s_2 \\ s_3 \end{bmatrix} \quad (3)$$

Thus the Stokes vector can be recovered from the measured intensities by dotting the inverse of the measurement matrix with the measured intensities,

$$\mathbf{S} = \mathbf{A}^{-1} \bullet \mathbf{I} = \mathbf{W} \bullet \mathbf{I} = \begin{bmatrix} 1.00 & 1.00 & 1.00 & 1.00 \\ 1.67 & 1.67 & -1.67 & -1.67 \\ -2.50 & 2.50 & 0.00 & 0.00 \\ 0.00 & 0.00 & -2.50 & 2.50 \end{bmatrix} \bullet \begin{bmatrix} i_{\text{path 1}} \\ i_{\text{path 2}} \\ i_{\text{path 3}} \\ i_{\text{path 4}} \end{bmatrix} \quad (4)$$

where  $\mathbf{W}$  is referred to as the data reduction matrix. It is the pseudo-inverse of the analyzer matrix. The measurement matrix of the system is determined through a series of measurements of known incident polarization states. The pseudo-inverse is chosen to invert the measurement matrix because this pseudo-inverse operation performs a least squares fit to an over-determined data set.

For this ideal system, the zero'th Stokes vector  $s_0$  (total intensity) is the sum of the measured intensities of all four paths. The first Stokes vector  $s_1$  is proportional to the difference between the sum of paths 1 and 2 and sum of paths 3 and 4. The second Stokes vector  $s_2$  is proportional to the measured intensity of path 1 minus the intensity of

path 2. Finally the third Stokes vector  $s_3$  is proportional to the intensity of path 4 minus the intensity of path 3.

Note that this analysis is done to summarize how data is reduced from the imaging polarimeter. The actual numbers in the data reduction matrix will be slightly different, since the polarization optics in the beam splitter block will not behave ideally.

### 3. Calibration Method

The calibration is done by launching a series of known polarization states into the entrance pupil of the imaging polarimeter. The optical setup for polarimetric calibration of the imaging polarimeter is shown in **Figure 2**. A tungsten-halogen lamp is collimated and the light is passed through a pair of 12mm apertures, 150mm apart. A Glan-Thompson polarizer is used to generate a horizontally polarized beam, establishing the coordinate system for the imaging polarimeter's polarimetric data products. The beam then passes through an achromatic linear retarder oriented at an angle  $\theta$ . The retardance of the retarder, measured in a separate step, is given in **Figure 3**.

Finally, the beam is diffused by a polarization preserving diffuser (the change in polarization state caused by the diffuser is less than 0.1%). The spot of light diffused by the diffuser is collimated by a 100mm EFL collimating lens, generating a uniformly polarized, uniformly illuminated object point at infinity. The imaging polarimeter objective is set to near infinity to form an image of the diffuser (slightly defocused to smear the pattern of the diffuser) on each of the four CCDs.

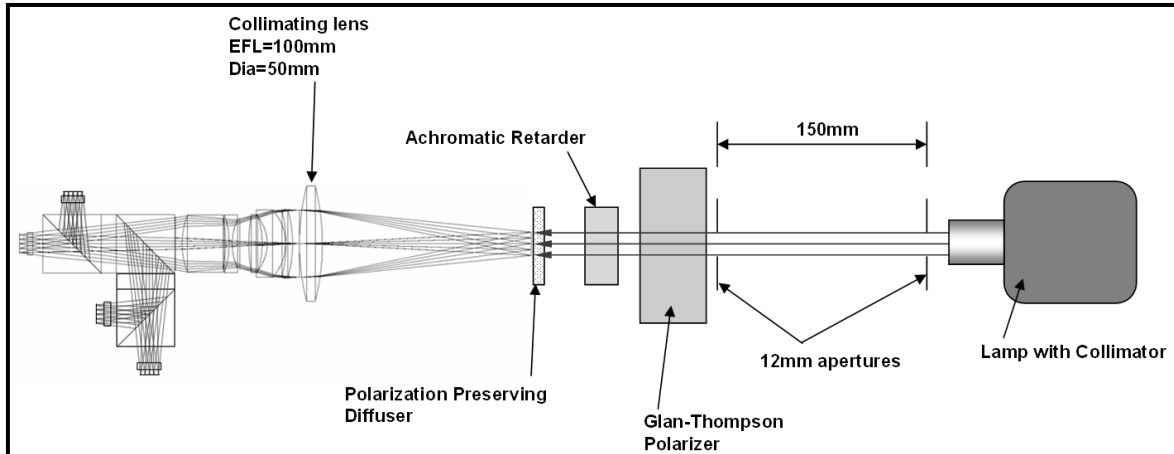


**Figure 2** Optical Schematic for Imaging Polarimeter Calibration.

The orientation of the retarder is rotated to introduce a set of known polarization states  $S_q$  sequentially into the polarimeter entrance aperture.

$$S_q = \begin{bmatrix} 1 \\ \cos^2(\theta) + \sin^2(\theta) \cdot \cos \delta \\ \sin(\theta) \cdot \cos(\theta) \cdot (1 - \cos \delta) \\ \sin(\theta) \cdot \sin \delta \end{bmatrix} \cdot i_{0,x,y} \quad (5)$$

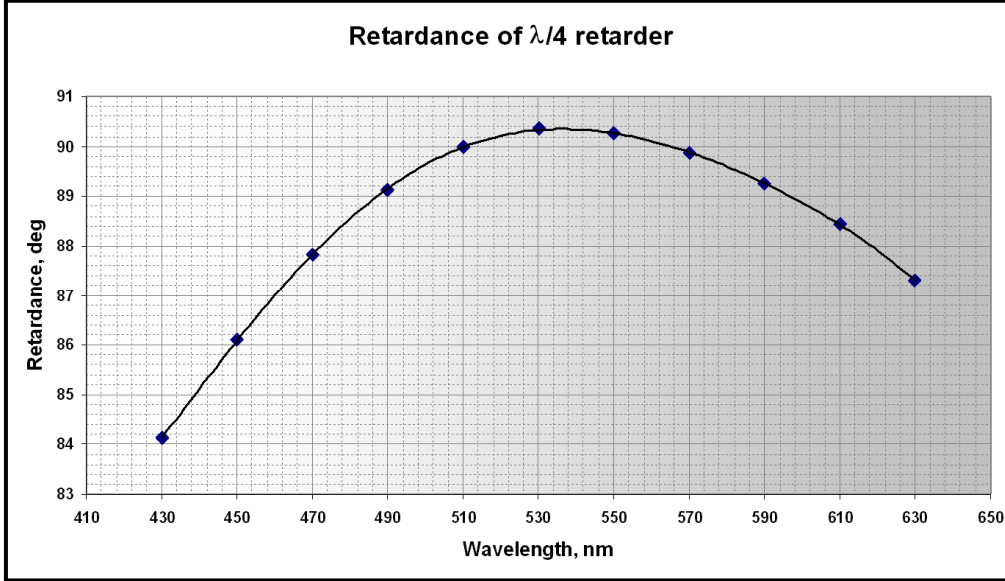


**Figure 3** Achromatic Retarder Retardance vs wavelength.

A set of Q images are captured at different orientations of the achromatic retarder. The following equation relates the known polarization states given in Equation 3 to measured pixel counts (ADU) at a given pixel location (x, y) on the CCD by the Analyzer matrix  $A$ .

$$\begin{bmatrix} c_{00} & c_{01} & c_{02} & \dots & c_{0Q} \\ c_{10} & c_{11} & c_{12} & \dots & c_{1Q} \\ c_{20} & c_{21} & c_{22} & \dots & c_{2Q} \\ c_{30} & c_{31} & c_{32} & \dots & c_{3Q} \end{bmatrix}_{x,y} = \begin{bmatrix} a_{00} & a_{01} & a_{02} & a_{03} \\ a_{10} & a_{11} & a_{12} & a_{13} \\ a_{20} & a_{21} & a_{22} & a_{23} \\ a_{30} & a_{31} & a_{32} & a_{33} \end{bmatrix}_{x,y} \cdot \begin{bmatrix} 1 & 1 & 1 & \dots & 1 \\ s_{1,0} & s_{1,1} & s_{1,2} & \dots & s_{1,Q} \\ s_{2,0} & s_{2,1} & s_{2,2} & \dots & s_{2,Q} \\ s_{3,0} & s_{3,1} & s_{3,2} & \dots & s_{3,Q} \end{bmatrix} \cdot i_{0,x,y} \quad (6)$$

$$\mathbf{C}_{x,y} = \mathbf{A}_{x,y} \cdot \mathbf{S} \cdot i_{0,x,y}$$

The data reduction matrix Analyzer matrix for a given pixel location (x,y), is then determined by the following equation,

$$\mathbf{A}_{x,y} = (\mathbf{S}^T \cdot \mathbf{S})^{-1} \cdot \mathbf{S}^T \cdot \mathbf{C}_{x,y} \cdot i_{0,x,y} \quad (7)$$

Finally, the data reduction matrix is given by,

$$\mathbf{D}_{x,y} = (\mathbf{A}^T \cdot \mathbf{A})^{-1} \cdot \mathbf{A}^T \quad (8)$$

The following equations compare the ideal Analyzer matrix to the actual measured Analyzer matrix for an axial object point,

$$\mathbf{A}_{ideal} = \begin{bmatrix} 0.250 & 0.150 & -0.200 & 0.000 \\ 0.250 & 0.150 & 0.200 & 0.000 \\ 0.250 & -0.150 & 0.000 & -0.200 \\ 0.250 & -0.150 & 0.000 & 0.200 \end{bmatrix} \quad \mathbf{A}_{actual} = \begin{bmatrix} 0.275 & 0.161 & -0.215 & -0.012 \\ 0.285 & 0.165 & 0.206 & 0.012 \\ 0.227 & -0.155 & 0.047 & -0.155 \\ 0.242 & -0.171 & -0.045 & 0.148 \end{bmatrix} \quad (9)$$

The following equations compare the ideal Data Reduction Matrix to the Actual Data Reduction Matrix

$$\mathbf{D}_{ideal} = \begin{bmatrix} 1.000 & 1.000 & 1.000 & 1.000 \\ 1.667 & 1.667 & -1.667 & -1.667 \\ -2.500 & 2.500 & 0.000 & 0.000 \\ 0.000 & 0.000 & -2.500 & 2.500 \end{bmatrix} \quad \mathbf{D}_{actual} = \begin{bmatrix} 0.950 & 0.992 & 0.950 & 0.992 \\ 1.366 & 1.426 & -1.628 & -1.700 \\ -2.369 & 2.298 & 0.188 & -0.187 \\ -0.703 & 0.724 & -3.380 & 3.105 \end{bmatrix} \quad (10)$$

## Results and Discussion

Several measurements were made in the laboratory and outdoors with the imaging polarimeter. First, measurements of know polarization states were made in order to check the calibration. **Figure 4** shows an example measurement of light emanating from an integrating sphere after passing through a linear polarizer oriented at 0 degrees. Light from the integrating sphere filled the entrance aperture of the system (f/2.8) and uniformly filled the entire FOV. The expected polarization is  $S=[1 \ 1 \ 0 \ 0]$ . A small variation (< 0.3%) from the expected polarization is observed across the field of view. Note the S1 image shown in the left hand side of **Figure 4** varies between 0.998 on the right of the image to 1.003 in the upper left of the image. The S2 image is on the right hand side of Figure 6 shows similar variation. Several other polarization states were checked yielding comparable accuracies.



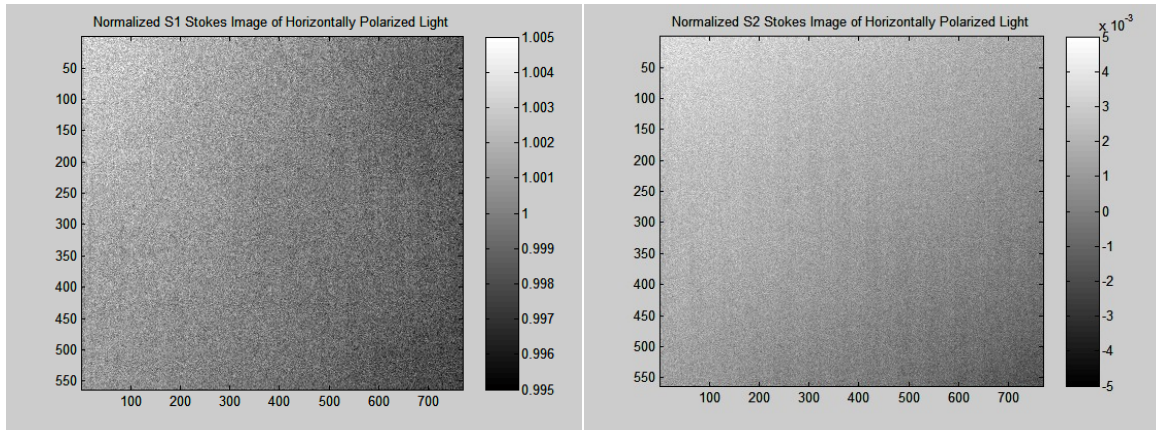


**Figure 4** Measured S1 and S2 of a uniformly horizontally polarized light from an integrating sphere.

**Figure 5** shows an optical setup to measure polarization reflected from a water surface. A 18"x36" black plastic grout pan was filled with water to a depth of approximately 3 inches. A white piece of foam core board was used as a reflecting light board. The board is front illuminated with a 500W Halogen lamp to produce a uniform un-polarized illumination of the water surface. The polarimeter is pointed toward the water at a 40 degree angle as shown.

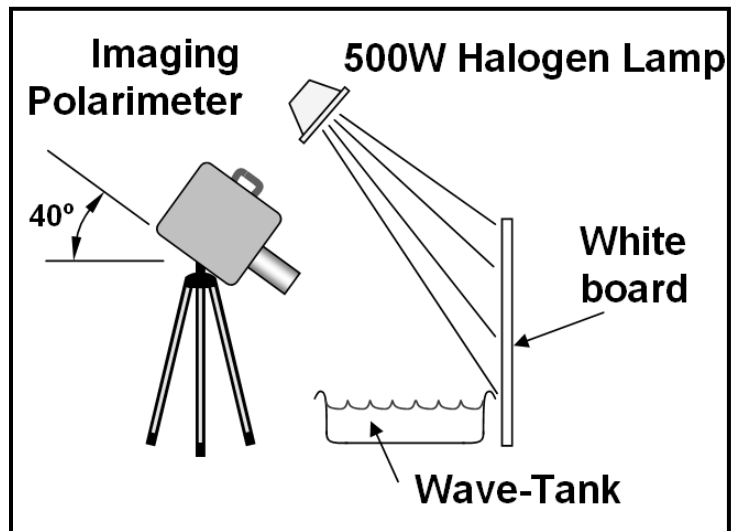


**Figure 5** Optical setup with wave-tank.

**Figure 6** shows the degree of linear polarization and the orientation of the polarization ellipse of a series of measurements taken of a water droplet in the wavetank. The integration time was set to 10ms and the camera was operated at 60 frames per second. The measurement illustrates the speed of the camera system in stopping the action of the water droplet. **Figure 7** shows the degree of polarization (DOP) of a single frame of the droplet. Note that the Degree of Polarization essentially equals the Degree of Linear Polarization because the Degree of Circular Polarization is zero.

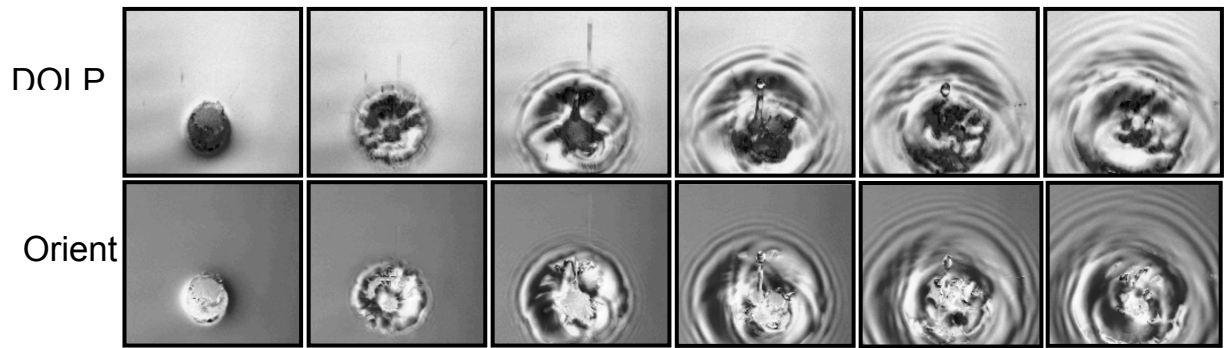


**Figure 6** Degree of linear polarization (DOLP) and Orientation of a water droplet.

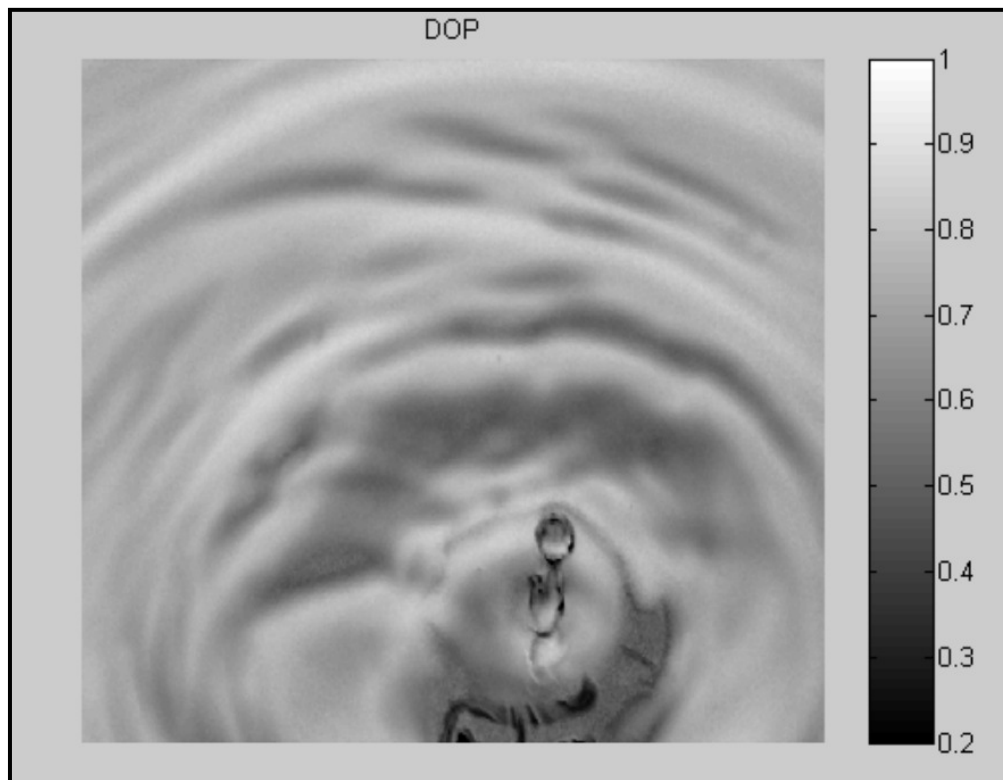


**Figure 7** Degree of linear polarization of water droplet.

The results appear to be quantitatively correct. First off, the measured DOLP component of the calm flat portion of the water measured to be 0.78. This is comparable to the expected value. **Figure 8** shows the DOLP of water (assuming a refractive index =1.33) calculated from the Fresnel equations. The DOLP of water at 40 degrees is approximately 0.8, which is good agreement considering the experimental error in setting the look angle of the polarimeter. The degree of linear polarization of the water surface at a number of other angles was measured with the imaging polarimeter with accuracies on the order a few percent error.

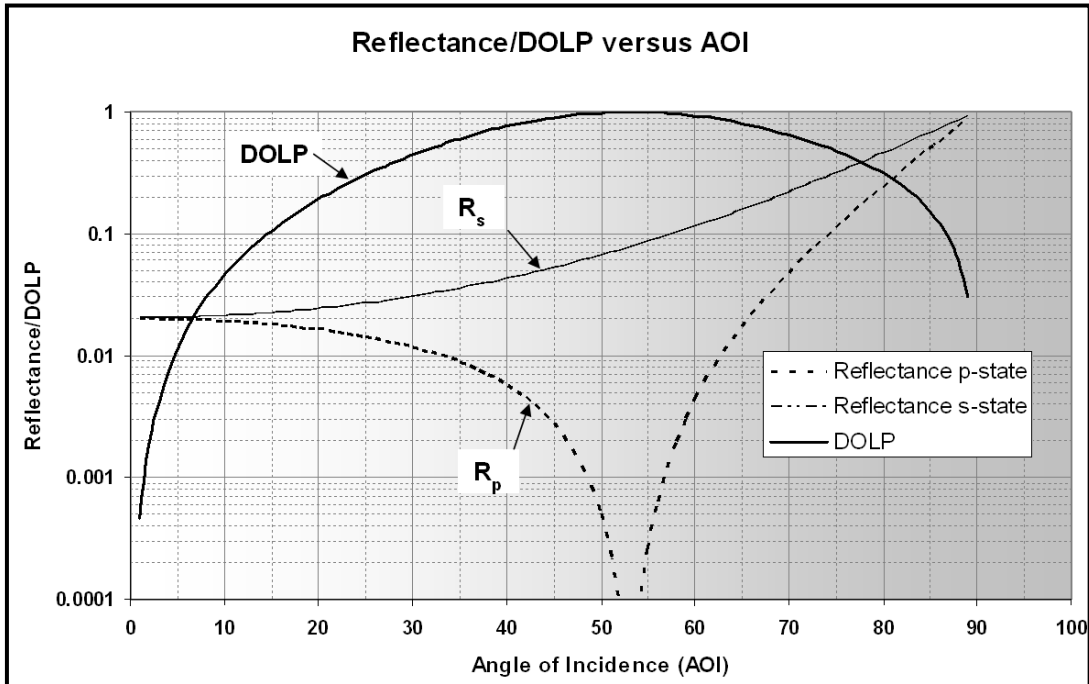


**Figure 8** Degree of linear polarization of the water surface.

Note that we have neglected the contribution to the measured polarization state that light reflected from the bottom of the wave-tank makes. We are justified in doing so here because the bottom of the tank is black. The surface of the water reflecting light from the bright white board is much brighter than the bottom of the wavetank. This is not always the case in shallow water situations or situations where sediments contribute to upwelling of light from the water surface. These contributions are a subject of current research, but are beyond the scope of this paper. For the purpose of this paper, we will consider surface reflection from the water only (no up-welling light and no thin-film layer on the surface of the water).

The orientation of linear polarization is defined as

$$\phi = \frac{1}{2} \cdot \tan^{-1} \left( \frac{S_2}{S_1} \right) \quad (11)$$

As long as the s-state reflectance is higher than the p-state reflectance, (which is normally the case for non-absorbing smooth surfaces) the orientation of linear

polarization is parallel with the s-state of reflected polarization. Thus for a water surface the relationship between linear polarization orientation and azimuthal wave-slope is straightforward. **Figure 9** shows the relationship between the s-state polarization and local orientation of wave-slope. Note that the angle  $\phi$  is perpendicular to the s-state. If the angles  $q$  and  $f$  are known, then the wave-slopes in the camera coordinates can be determined. This relationship between  $\theta$ ,  $\phi$  and wave-slope has been described before by Shultz et.al.<sup>2</sup> If the look angles of the polarimeter relative to the water surface are known, then finding the wave-slope angles relative to earth coordinates is straight-forward.

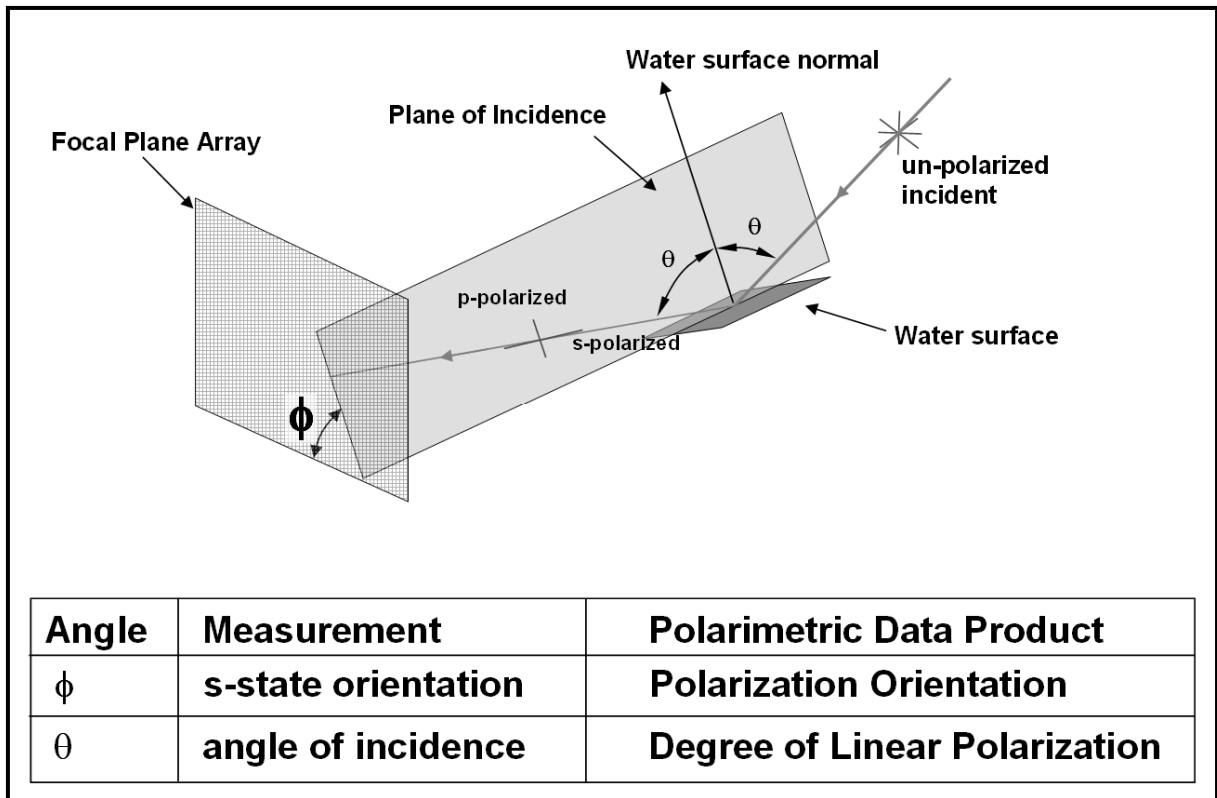


**Figure 9** Relationship between water surface, angle of incidence and orientation of linear polarization.

**Figure 10** shows the imaging polarimeter mounted to a boom over-looking the water surface at Scripps Pier in LaJolla, California. The measurements were done by Howard Schultz, University of Massachusetts Professor in Computer Engineering department. Several gigabyte movies of ocean waves were collected over a 2 week period. A few of these movies were played at the conference session. **Figure 13** shows a single image of  $S_0$  (intensity), degree of linear polarization and X and Y wave-slope normals (in units of degrees) of a breaking wave. Wave-slope angles X and Y of zero indicate that the wave is in the surface of the page (horizontal to earth). A positive or negative Y component indicates that wave is tilted toward the top of the page or the bottom of the page. A positive or negative X slope indicates that the wave is tilted to the right or the left of the page.

The measurements appear qualitatively correct. The wave breaks from the top of the page toward the bottom of the page. Note on the Y-component image shows that the trailing side of the wave has a positive slope and the leading portion of the wave has a negative slope as expected.

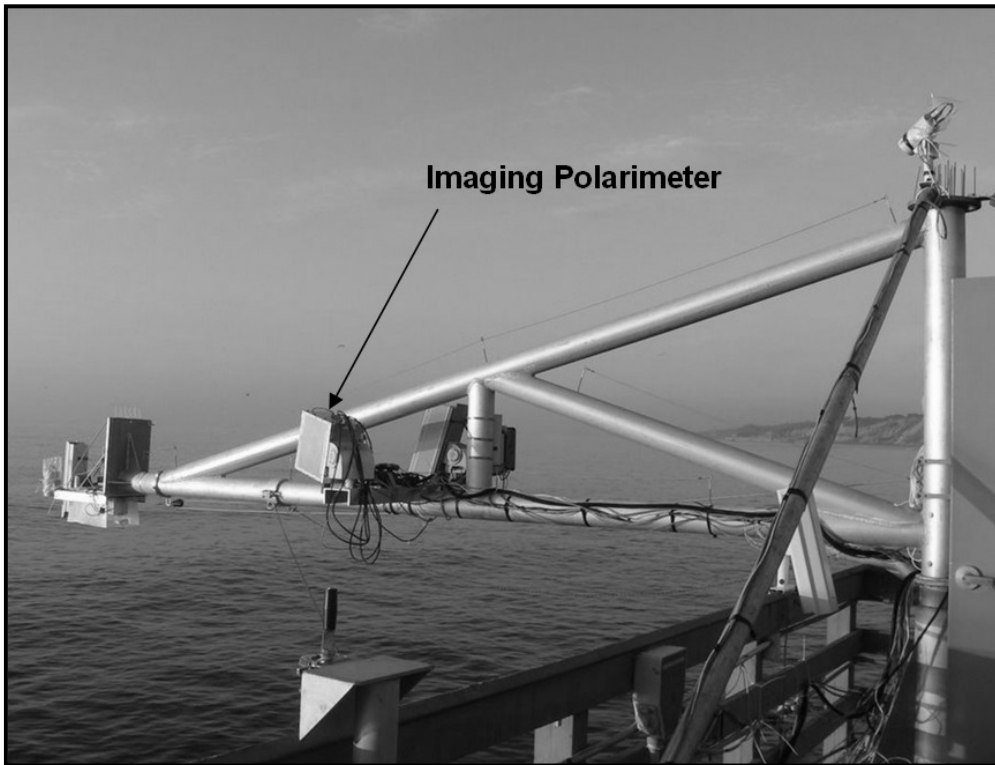


**Figure 10** Imaging Polarimeter mounted to boom at Scripps Pier.

## Summary and Next Steps for Research

The imaging polarimeter is a good tool for accurately monitoring water waves-slopes in real-time. The wave-slope resolution is approximately 1 degree wave-slope. The integration time for the measurements can be as short as 1 ms, this is sufficiently short to effectively freeze the motion of the wave. The camera can operate at frame rates as high as 60 frames per second. For stand-off distances of 8 meters above the water surface the spatial resolution of the images (instantaneous field of view) are approximately 2mm.

The effects of light upwelling from beneath the water and the effect of background sky polarization have been neglected in this study. In the next phase of this research, these issues will be addressed. We currently believe that for many situations, the effects of sky polarization and light upwelling can be ignored without significant impact to the accuracy of the data. Our future research will take a two phase approach. First, we will generate an emulator in software that will produce data sets simulating

these effects and the corresponding data reduction algorithms to separate the effects. Second, a wave-tank is currently being constructed at the University of Massachusetts that will allow us to systematically generate these effects. Measurements will be made of simple waves in the wave-tank with the imaging polarimeter. The polarimetric data will be mapped to wave-slope quantities using our data reduction algorithms. The output of the imaging polarimeter will be compared to mechanical wave-probe outputs.

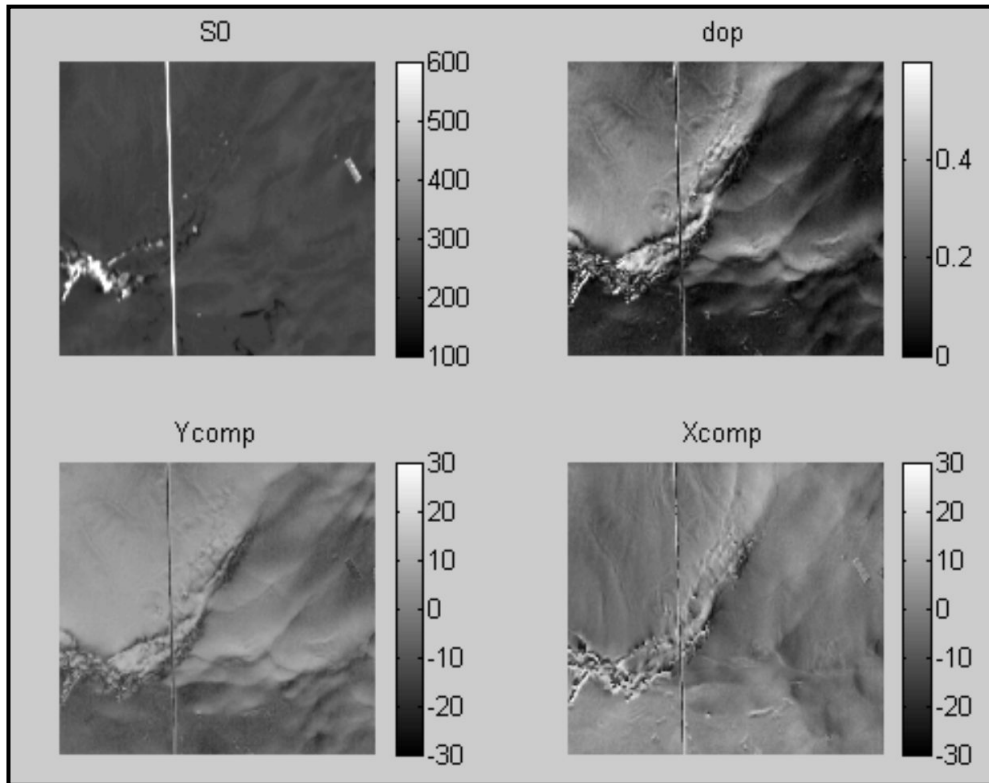


**Figure 11** S0, DOP, X and Y surface normals (in degrees) of wave-slopes.

Acknowledgements:

**This work was funded by the Office of Naval Research grant numbers:  
N00014-06-1-0956 and N00014-07-1-0731**

<sup>1</sup> J. Larry Pezzaniti, David Chenault, Mike Roche, John Reinhardt, Joseph P. Pezzaniti, and Howard Schultz, "Four Camera Complete Stokes Imaging Polarimeter," Proc. SPIE 6972, March 2008.

<sup>2</sup> Howard Schultz, Chris J. Zappa, Michael L. Banner, Andrés Corrada-Emmanuel and Larry Pezzaniti "A Method for Recovering the Two-dimensional slope field of the Ocean Surface Waves Using an Imaging Polarimeter," presented at the 2008 Ocean Sciences Meeting, Orlando, FL March 2-7, 2008.